Bioorganic & Medicinal Chemistry Letters xxx (xxxx) xxx–xxx

Contents lists available at ScienceDirect

Bioorganic & Medicinal Chemistry Letters

journal homepage: www.elsevier.com/locate/bmcl

PEGylated cyanine dye nanoparticles as photothermal agents for mosquito and cancer cell control

Qi Xu[a], Yujun Shen[a], Yongchao Zhang[a], Xusheng Shao[a,b,*]

[a] Shanghai Key Laboratory of Chemical Biology, School of Pharmacy, East China University of Science and Technology, Shanghai 200237, China
[b] State Key Laboratory of Bioreactor Engineering, East China University of Science and Technology, Shanghai 200237, China

ARTICLE INFO

Keywords:
Photothermal
Nanoparticles
PEGylated
Phototoxic activity
Mosquito larvae

ABSTRACT

Conversion of light energy to heat via photothermal conversion agents (PTCAs) is of great interest and has potential applications. Here, we described a heptamethine cyanine (Cy7) dye nanoparticles (Cy7-PEG NPs) prepared from heptamethine cyanine and poly(ethylene glycol) (PEG400) via a simple solvothermal process as novel PTCA. Cy7-PEG NPs have absorption maximum at about 808 nm and good photothermal conversion ability. Upon irradiation, Cy7-PEG NPs can effectively kill living mosquito larva (*Aedes albopictus*) through heat generation. Furthermore, Cy7-PEG NPs have excellent phototoxic activity to Sf9, HeLa and MCF-7 cells. Our results indicated that Cy7-PEG NPs can be used as controlling agent for mosquito larvae and cancer cells.

Photothermal conversion agents (PCTAs) attract extensive attentions recently among scientists.[1–3] PCTAs are a kind of materials that can convert light energy to heat under near infrared (NIR) irradiation.[4] PCTAs are widely used as therapeutic agents for cancer and bacteria control due to their excellent specificity, spatiotemporal controllability, less side effects and greater tissue penetration capacity of NIR light.[4] They can raise the cell local temperature and induce local eradication of tumor cells or bacteria.[5–7] The commonly-used PCTAs are inorganic nanomaterials such as Au-based nanoparticles (NPs),[8–12] nanocarbons[13–16] and transition-metal nanomaterials.[17–20] As most inorganic nanomaterials are nonbiodegradable and difficult to diffuse throughout tissues, organic PCTAs have been developed in recent years as replacements of inorganic counterparts owing to their biodegradability and easy structural modification merits.[21–29]

The heptamethine cyanines (Cy7) generally show absorption in the NIR region, longer wavelengths of light can penetrate cells and tissues more easily and are not absorbed by other biomolecules in the cell.[30] Many NIR cyanine dyes have been developed as both PCTAs and imaging agents for tumor treatment.[31–35] However, rapid decomposition, low hydrophilicity and poor photostability impede their applications in cancer therapy. To enhance the photothermal conversion and therapeutic efficiency, Cy7 dyes-containing nanoparticles are usually prepared via chemical conjugation or encapsulation.

In this work, we constructed a novel NIR Cy7-based NPs for the control of mosquito larvae and cancer cells. Our NIR Cy7 dye was designed and prepared by introducing *p*-tolylthio-substituent with a view to enhancing the conjugation and bathochromic shift of the absorption. Encapsulation to poly(ethylene glycol) (PEG400) can improve hydrophilicity of NIR Cy7. Since living organisms are sensitive to temperature changes, which is similar with human fever, we envisioned that the temperature evaluation can lead to malfunction of physiological processes, tissue damage, and eventual organism death. To the best of our knowledge, phototoxic effects of PCTAs have never been evaluated on living insects. We studied here for the first time the application of PCTAs in photothermally killing the mosquito larvae.

The synthetic route of Cy7 dye and its nanoparticles were depicted in Fig. 1. Originally, dye CyOH was prepared according to the previously-reported procedure, then CyOH and 4-methylbenzenethiol are catalyzed by triethylamine (TEA) to form the target dye Cy7. After purification by silica gel column chromatography, Cy7 was characterized by proton nuclear magnetic resonance (^{1}H NMR) and carbon-13 magnetic resonance (^{13}C NMR) and electrospray mass spectrometry (ESI-MS). Cy7-PEG NPs was prepared by means of a solvothermal method, ethanol solution of PEG400 (0.5 g) and compound Cy7 (30 mg) was heated with stirring at 160 °C for 2 h. After cooling down to room temperature, the crude product was transferred to a dialysis bag, then

* Corresponding author.
E-mail address: shaoxusheng@ecust.edu.cn (X. Shao).

https://doi.org/10.1016/j.bmcl.2019.05.057
Received 14 December 2018; Received in revised form 15 May 2019; Accepted 29 May 2019
0960-894X/

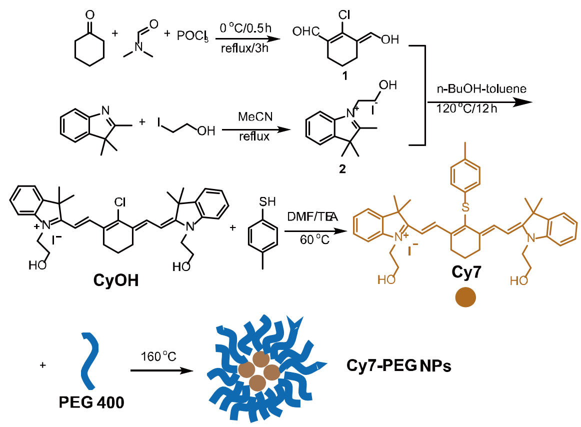

Fig. 1. Synthetic route of Cy7 and preparation of Cy7-PEG NPs.

the dialysis bag was transferred to a freeze drier for freeze-drying to afford green-yellow solid powder.

The morphology of our Cy7-PEG NPs was characterized by transmission electron microscopy (TEM) (Fig. 2A). For TEM samples preparation, the Cy7-PEG NPs dispersions dropped on conventional TEM copper grids and dried in air. Cy7-PEG NPs showed spherical structures, uniform shapes and good dispersion, indicating successful preparation of the expected NPs. The particles size distribution of Cy7-PEG NPs was measured by dynamic light scattering. The NPs all show a sphere-like shape with an average size of 164.06 ± 12.5 nm (Fig. 2B). The absorption spectra of Cy7 and Cy7-PEG NPs in DMSO was presented in Fig. 2C. The absorption maximum is at about 808 nm, which located in the near infrared region. The Cy7 content in Cy7-PEG NPs was determined using UV–Vis standard curve (Fig. 2D) providing the load rate of 12.4% wt%.

The powder of Cy7-PEG NPs was dissolved in ethanol and analyzed with a UV–vis spectrophotometer at 796 nm by using a standard curve method. The linear relationship between the concentration of Cy7-PEG NPs and absorption intensity at 796 nm in ethanol was presented in Fig. 2D. The drug loading content (DLC) was calculated to be 5.3% by the following equation:

$$\mathrm{DLC(wt\%)} = \text{the weight of Cy7 in Cy7 - PEG NPs/the weight Cy7 - PEG NPs}$$

The photostability of Cy7-PEG NPs was investigated by monitoring their absorbance changes upon continuous laser irradiation at a power of 4.0 W cm^{-2} for different time periods. I_0 is the maximum absorbance of Cy7-PEG NPs in the NIR region, and I is the absorbance of Cy7-PEG NPs after different irradiation periods. As shown in Fig. 2E, no obvious absorbance decay was observed for Cy7-PEG NPs, indicating that Cy7-PEG NPs has good photostability.

The photothermal conversion ability of Cy7-PEG NPs was evaluated in aqueous solution. Temperature changes curves was recorded under irradiation of 300 s, various aqueous concentrations (100, 50, 25, 12.5, 0 μg mL^{-1}) of Cy7-PEG NPs were prepared and tested. Dramatic temperature evaluation occurred during irradiation and maximum ΔT approached 41.2 °C at concentration of 100 μg mL^{-1} (Fig. 3A). The temperature of pure water maintained almost unchanged after laser irradiation, only 2.81 °C temperature evaluation was detected in pure water. The temperature increased with the prolongation of illumination and reached steady state after about 230 s irradiation, indicating a balance between light energy absorbing and heat releasing. When the concentration was fixed at 25 μg mL^{-1}, the temperature evaluation rate increased with the increase of irradiation power (Fig. 3B). The above results indicated that Cy7-PEG NPs can efficiently convert light energy to heat. Photothermal conversion efficiency (η) is an important index that indicated the ability of utilizing light energy. This index was calculated referring to the method reported previously.[36] Photothermal conversion efficiency of our NPs is about 33.4% under 808 nm laser irradiation. After reaching steady-state, thermal exchange from the solution to environment was also monitored (Fig. 3C).

With successful identification of excellent photothermal ability of Cy7-PEG NPs, we then investigated their ability in killing mosquito larvae (*Aedes albopictus*) through heat generation. All the previously-reported applications of PCTAs mainly focused on cells or tissues, but seldom on living organisms. We used mosquito larvae as living animal here for investigation. Mosquito is a main sanitary insect pest that transmits many deadly diseases and causes bite allergy. Mosquito larva were firstly co-incubated with Cy7-PEG NPs for 4 h and then irradiated with laser light of different power and the mortality was recorded at different time intervals (Fig. 4A and B). The photothermal killing effects on mosquito larvae increased with the increase of laser illumination time or NPs concentration, indicating that the mortality correlated closely with the amount of heat generation. Laser irradiation or Cy7-PEG NPs alone did not have any influence on the larvae. These results demonstrated that the heat production was the main factor that led to the death of mosquito larvae. Median lethal concentrations (LC_{50}) were 120 μg mL^{-1} and 75.4 μg mL^{-1} under laser power density of 6 W cm^{-2} and 8 W cm^{-2}, respectively.

We further evaluated phototoxic effects of Cy7-PEG NPs on Sf9 cells (Spodoptera frugiperda cells) (Fig. 5A). As comparison, Cy7 and Cy7-PEG NPs with or without irradiation were screened using MTT assay at light intensity of 4 W cm^{-2}. When treated with Cy7 alone, cell viability decreased significantly even at concentration of 5 μg mL^{-1} and the LC_{50} value was 0.62 μg mL^{-1}. When Cy7 was encapsulated, its intrinsic toxicity in the dark reduced 4-folds with LC_{50} approaching 2.51 μg mL^{-1}. When co-treated with Cy7-PEG NPs and laser light, phototoxicity towards Sf9 cells (IC_{50} = 0.0048 μg mL^{-1}) enhanced around 500-folds compared to the dark control. Sole laser illumination had no apparent impact on cell survival. All above observations proved that the phototoxicity of Cy7-PEG NPs to cells can be triggered by light.

As PCTAs draw tremendous attention in cancer treatment,[37] the ability of Cy7-PEG NPs in ablating HeLa (human cervical carcinoma) and MCF-7 (human breast adenocarcinoma) cells was studied (Fig. 5B and C). HeLa or MCF-7 cells were subjected to various concentrations of Cy7-PEG NPs and irradiated with laser light (4 W cm^{-2} for 3 min) or kept in the dark. Without irradiation, Cy7-PEG NPs had dark toxicity to both HeLa and MCF-7 cells, which can inhibit around 60% cell viability at 5 μg mL^{-1}. The IC_{50} values are 0.43 μg mL^{-1} and 0.30 μg mL^{-1} towards HeLa and MCF-7 cells, respectively. Upon light illumination, the

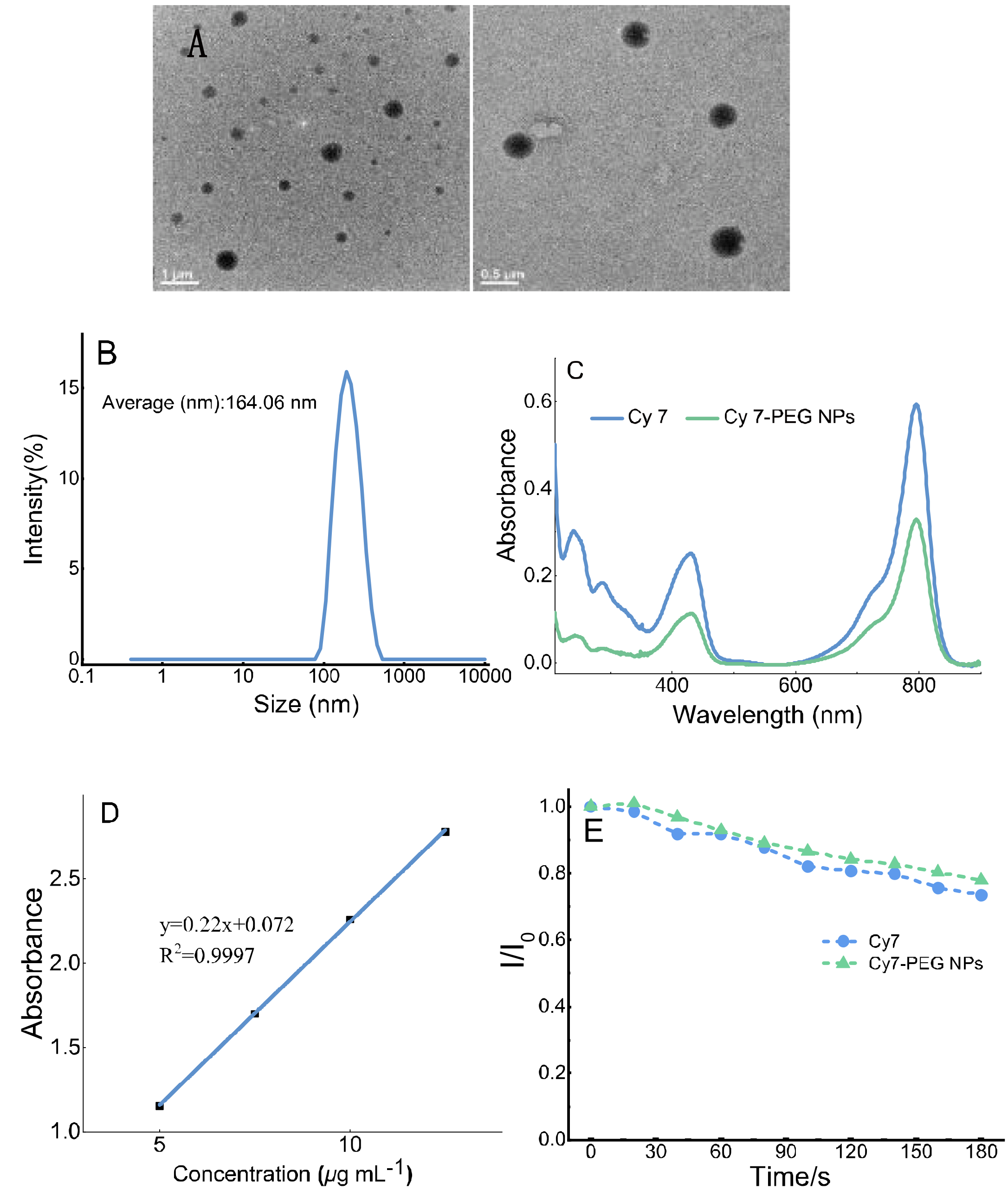

Fig. 2. (A) Transmission electron microscopy (TEM) images of Cy7-PEG NPs; (B) The diameter distribution of TEM image; (C) UV–Vis spectra of Cy7 and Cy7-PEG NPs in ethanol. (D) The linear relationship between the concentration of Cy7-PEG NPs and absorption intensity at 796 nm in ethanol, the linear range is 5.0–15 μg mL^{-1} (R^2 = 0.9997) and the regression equation is y = 0.22x + 0.07. (E)Absorbance evolution of Cy7 and Cy7-PEG NPS (5 μg mL^{-1}) upon continuous laser irradiation (808 nm, 4.0 W/cm^{-2}) for different time periods, where I0 is the maximum absorbance of Cy7 and Cy7-PEG NPs in the NIR region and I is that of Cy7 and Cy7-PEG NPs after irradiation for different time periods.

activity increased significantly about 693- (HeLa cells) and 15-fold (MCF-7 cells) in comparison with the dark controls. Data shown in the study were obtained from at least three independent experiments and expressed as mean ± standard deviation (S.D.). Significance was assessed by *t*-test. Difference significance between light group vs. the same concentration of dark group was assessed as $^*p < 0.05$;

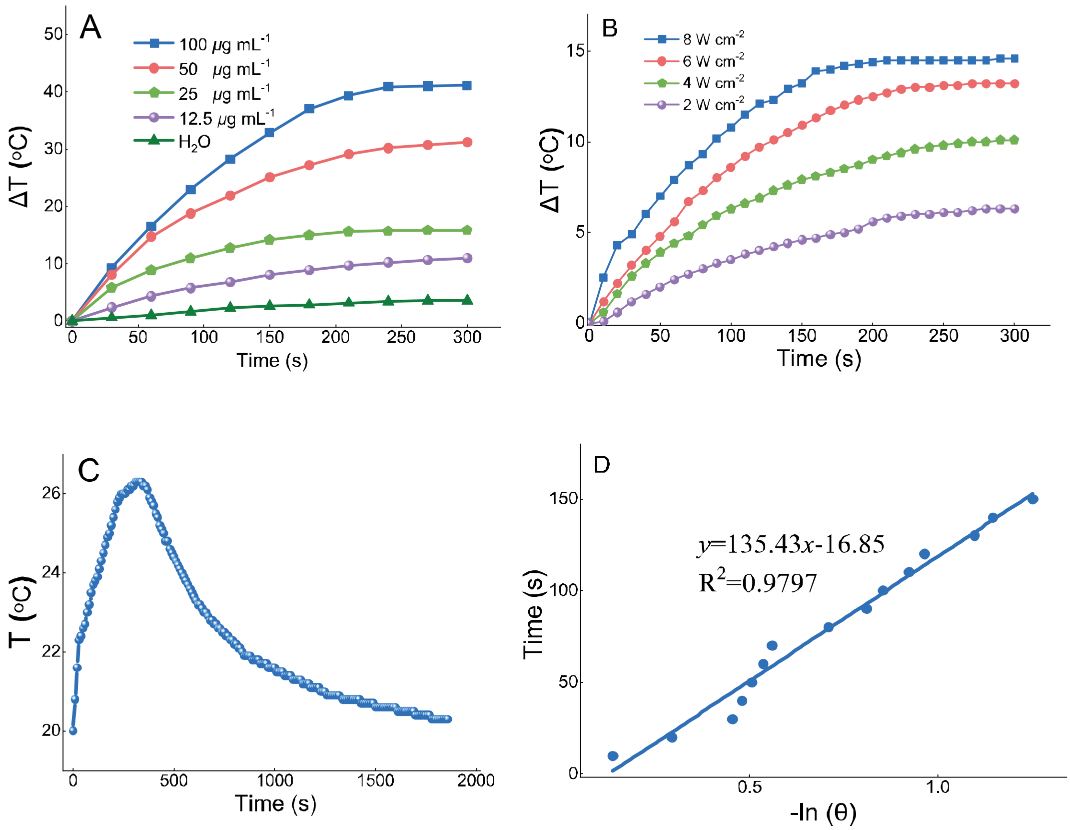

Fig. 3. (A) Temperature evaluation of various concentrations of Cy7-PEG NPs aqueous solution (0, 12.5, 25, 50, 100 μg mL^{-1}) under laser power density of 6 W cm^{-2}; (B) Temperature change of Cy7-PEG NPs aqueous solution (25 μg mL^{-1}) irradiated by various laser power density (808 nm, 2, 4, 6, 8 W cm^{-2}); (C) Photothermal profile of Cy7-PEG NPs aqueous solution (50 μg mL^{-1}) irradiated by laser light to reach steady state, followed by natural cooling to room temperature; (D) Plot of cooling time versus negative natural logarithm of the temperature driving force obtained during the cooling period.

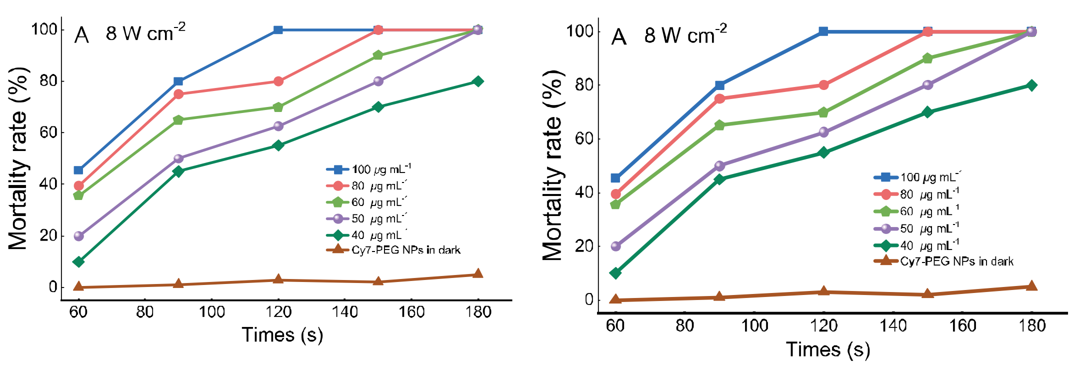

Fig. 4. Photothermal effect of Cy7-PEG NPs against *Aedes albopictus* larvae irradiated at laser power density of 8 W cm^{-2} (A) and 6 W cm^{-2} (B), respectively.

$^{**}p < 0.01$; $^{***}p < 0.001$.

Trypan blue staining experiment was performed to visually discriminate the viable and nonviable cells. For all three tested cells, only light or Cy7-PEG NPs (1 μg mL^{-1}) cannot cause any damage to the cells, while cells treated by light plus Cy7-PEG NPs became nonviable (a distinctive blue color appeared in dead cells) (Fig. 6). This trend was

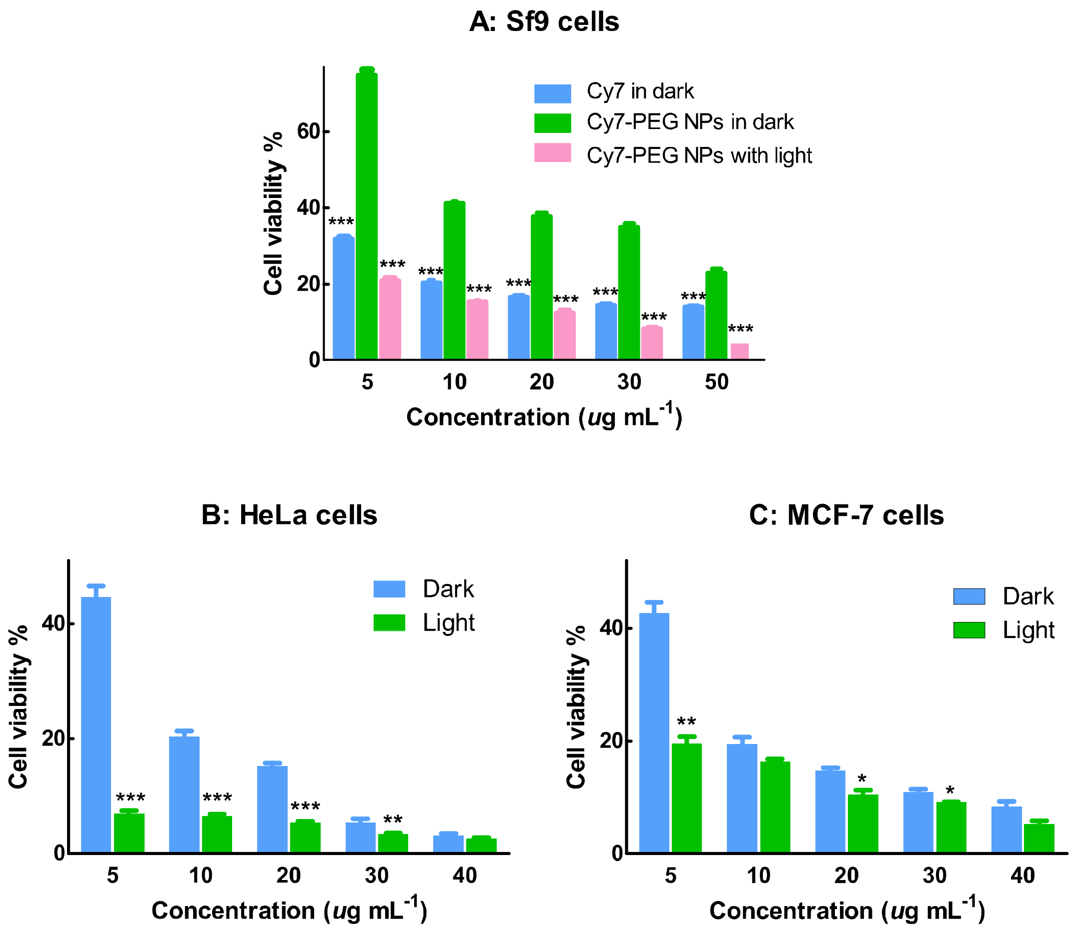

Fig. 5. Cytotoxicity curves of compound Cy7 and Cy7-PEG NPs towards Sf9 cells (A), HeLa cell (B) and MCF-7 cells (C), respectively, irradiated by laser intensity of 4 W cm^{-2} for 3 min. Data mentioned above are represented as the mean ± S.D. (n ≤ 4 per group). *, $p < 0.05$; **, $p < 0.01$; ***, $p < 0.001$ vs. the the same concentration of dark group condition.

further verified by fluorescence staining studies using fluorescent calcein-AM (green) and propidium iodide (red) on three cells (Fig. 6), suggesting that the toxicity of Cy7-PEG NPs towards cells showed a light-dependent behavior.

In conclusion, a novel cyanine dye Cy7 whose maximum absorption wavelength bathochromically shifted to about 808 nm was prepared by introducing *p*-tolylthio-substituent. Cy7 encapsulated to PEG400 afforded a cyanide-based nanoparticles with photothermal conversion efficiency approaching 33.4%. Using the heat generated upon 808 nm light irradiation, the prepared nanoparticles have photothermally lethal effect on mosquito larvae whose LC_{50} value is 75.4 μg mL^{-1} under laser power of 8 W cm^{-2}. The good photothermal properties of Cy7 nanoparticles also allowed of light-dependent control of HeLa and MCF-7 cells. When irradiated with laser light (4 W cm^{-2}) for 3 min, the IC_{50} values were 0.43 μg mL^{-1} and 0.30 μg mL^{-1} towards HeLa and MCF-7 cells, respectively. Our Cy7-PEG NPs provide an alternative potential PCTA for mosquito control and photothermal therapy.

Acknowledgments

This work was financial supported by National Key Research and Development Program of China (2018YFD0200100), National Natural Science Foundation of China (No. 21877039), Science and Technology Commission of Shanghai Municipality (16391902300) and Innovation Program of Shanghai Municipal Education Commission (2017-01-07-00-02-E00037).

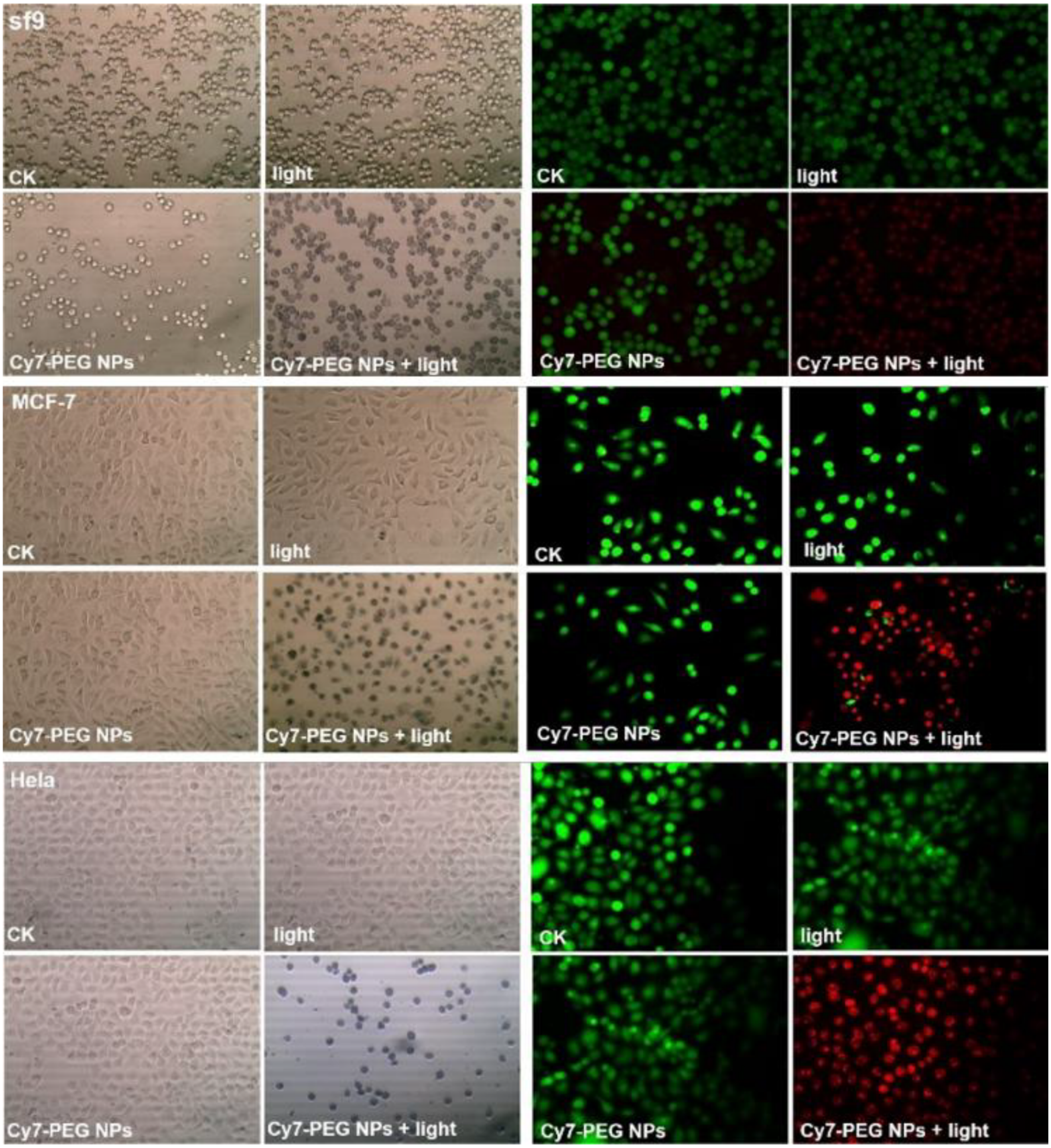

Fig. 6. Microscopy and fluorescence images of Sf9, HeLa, and MCF-7 cells treated by light, Cy7-PEG NPs or Cy7-PEG NPs plus light (808 nm and 4 W cm^{-2} for 3 min) and then stained by trypan blue, calcein-AM and propidium iodide.

Appendix A. Supplementary data

Supplementary data to this article can be found online at https://doi.org/10.1016/j.bmcl.2019.05.057.

References

1. Zhang X, Sun B, Zuo S, et al. *ACS Appl Mater Interfaces.* 2018;10:30155–30162.
2. Ai X, Mu J, Xing B. *Theranostics.* 2016;6:2439–2457.
3. Alkilany AM, Thompson LB, Boulos SP, Sisco PN, Murphy CJ. *Adv Drug Deliv Rev.* 2012;64:190–199.
4. Liu Y, Bhattarai P, Dai Z, Chen X. *Chem Soc Rev.* 2018. https://doi.org/10.1039/C8CS00618K.
5. Pereyra JY, Cuello EA, Salavagione HJ, Barbero CA, Acevedo DF, Yslas EI. *Photodiagn Photodyn.* 2018;24:36–43.
6. Shanmugam V, Selvakumar S, Yeh C-S. *Chem Soc Rev.* 2014;43:6254–6287.
7. Wu M-C, Deokar AR, Liao J-H, Shih P-Y, Ling Y-C. *ACS Nano.* 2013;7:1281–1290.
8. Liu Y, Zhang X, Luo L, et al. *ACS Biomater Sci Eng.* 2018;4:2911–2921.
9. Liu Y, Yang Z, Huang X, et al. *ACS Nano.* 2018;12:8129–8137.
10. Parchur AK, Sharma G, Jagtap JM, et al. *ACS Nano.* 2018;12:6597–6611.

11. Yang L, Tseng Y-T, Suo G, et al. *ACS Appl Mater Interfaces.* 2015;7:5097–5106.
12. Vijayaraghavan P, Liu C-H, Vankayala R, Chiang C-S, Hwang KC. *Adv Mater.* 2014;26:6689–6695.
13. Hu S-H, Fang R-H, Chen Y-W, Liao B-J, Chen IW, Chen S-Y. *Adv Funct Mater.* 2014;24:4144–4155.
14. Yi DH, Yoo HJ, Mahapatra SS, Kim YA, Cho JW. *J Colloid Interfaces Sci.* 2014;432:128–134.
15. Li Q, Ruan H, Li H. *Pharm Nanotechnol.* 2014;2:58–64.
16. Liu Z, Liang X-J. *Theranostics.* 2012;2:235–237.
17. Zhao Y, Cai Q, Qi W, et al. *ChemistrySelect.* 2018;3:9510–9516.
18. Li K-C, Chu H-C, Lin Y, Tuan H-Y, Hu Y-C, Appl ACS. *ACS Appl Mater Interfaces.* 2016;8:12082–12090.
19. Chou SS, Kaehr B, Kim J, et al. *Angew Chem.* 2013;125:4254–4258.
20. Fu G, Liu W, Feng S, Yue X. *Chem Commun.* 2012;48:11567–11569.
21. Jung HS, Verwilst P, Sharma A, Shin J, Sessler JL, Kim JS. *Chem Soc Rev.* 2018;47:2280–2297.
22. Lu Z, Huang F-Y, Cao R, et al. *ACS Appl Mater Interfaces.* 2018;10:26028–26038.
23. Zong S, Wang X, Lin W, Liu S, Zhang W. *Bioconjug Chem.* 2018;29:2619–2627.
24. Yang Z, Ren J, Ye Z, et al. *J Mater Chem B.* 2017;5:1108–1116.
25. Zhou B, Li Y, Niu G, et al. *ACS Appl Mater Interfaces.* 2016;8:29899–29905.
26. Wang J, Qiu J. *Cancer Res Front.* 2016;2:67–84.
27. Song X, Chen Q, Liu Z. *Nano Res.* 2015;8:340–354.
28. Zha Z, Yue X, Ren Q, Dai Z. *Adv Mater.* 2012;25:777–782.
29. Yang J, Choi J, Bang D, et al. *Angew Chem-Int Edit.* 2010;50:441–444.
30. Shindy HA. *Dyes Pigm.* 2017;145:505–513.
31. Mindan L, Ning K, Chuan C, et al. *Nanotechnology.* 2017;28:445710.
32. Lee S, George Thomas R, Ju Moon M, et al. *Sci Rep.* 2017;7:2108.
33. Zhang J, Liu S, Hu X, Xie Z, Jing X. *ACS Biomater Sci Eng.* 2016;2:1942–1950.
34. Lin W, Li Y, Zhang W, et al. *ACS Appl Mater Interfaces.* 2016;8:24426–24432.
35. Zheng M, Li Y, Liu S, et al. *ACS Appl Mater Interfaces.* 2016;8:23533–23541.
36. Svaasand LO, Gomer CJ, Morinelli E. *Laser Med Sci.* 1990;5:121–128.
37. Melamed JR, Edelstein RS, Day ES. *ACS Nano.* 2015;9:6–11.